ELSEVIER

Journal of Organometallic Chemistry 485 (1995) 45–53

Journal of Organometallic Chemistry

Organotin(IV) polypyrazolylborates VII. Hydridotris(3,4,5-trimethyl-1*H*-pyrazol-1-yl)borates. X-ray crystal structures of $K(HB(3,4,5\text{-}Me_3Pz)_3]$ and $[HB(3,4,5\text{-}Me_3Pz)_3\ SnMeCl_2]$

Giancarlo Gioia Lobbia [a,*], Patrizio Cecchi [b], Riccardo Spagna [c], Marcello Colapietro [d], Augusto Pifferi [c], Claudio Pettinari [a]

[a] *Dipartimento di Scienze Chimiche, Università di Camerino, Via S. Agostino 1, I-62032 Camerino, Italy*
[b] *Dipartimento di Agrobiologia ed Agrochimica, Università della Tuscia, Via S.C. De Lellis, I-101100 Viterbo, Italy*
[c] *Istituto di Strutturistica Chimica "G. Giacomello" CNR, CP10 00016 Monterotondo Stazione, Roma, Italy*
[d] *Dipartimento di Chimica, Università di Roma "La Sapienza" P.le A. Moro, 8, 00100 Roma, Italy*

Received 28 February 1994

Abstract

Tin(IV) and organotin(IV) compounds containing hydridotris(3,4,5-trimethyl-1*H*-pyrazol-1-yl)borate (L^3), $[R_nSnCl_{4-n-1}L^3]$ (R = Me, n = 0-2) have been synthesised and studied by NMR (^1H, ^{13}C, ^{119}Sn) spectroscopic techniques. The compounds are not fluxional and contain six-coordinate tin(IV) with a tridentate ligand. X-ray crystal structure of $[MeSnCl_2L^3]$ is reported together with that of the parent potassium hydridotris(3,4,5-trimethyl-1*H*-pyrazol-1-yl)borate, $K(C_{18}H_{28}N_6B)$ and comparisons are made.

Keywords: Boron; Tin; Pyrazolylborates; X-ray

1. Introduction

Tris(pyrazolyl)borates L{$[HB(Pz)_3]^-$ or *C*-substituted $[HB(pz)_3]^-$, Pz = 1*H*-pyrazol-1-yl} constitute a class of unique uninegative tridentate ligands possessing virtual C_{3v} symmetry. They have been successfully combined into a huge number of complexes, mainly with organo-transition metal ions. Trofimenko introduced them in the sixties and has regularly contributed to and reviewed exhaustively the subject [1].

Post-transition metal derivatives (d^{10} species) in particular tin [2] with these same ligands have been much less investigated. In earlier papers several mercury [3] and tin(IV) [4] complexes [R(or X)-HgL] or $[R_nCl_{4-n-1}SnL]$ were described, [L is L^0 (pz = Pz), L^1 (pz = 3-MePz), L^2 (pz = 3,5-Me_2Pz), R = alkyl or phenyl, X = halide, pseudohalide, or mercaptide, n = 0-2].

The ion L^3 (pz = 3,4,5-Me_3Pz), whose crystal structure as the potassium salt is reported here, has been rarely studied since its introduction [5]. These are Mössbauer and structural studies [6a,b], and a mechanistic and theoretical study in catalysis [6c]. We wished to investigate the interplay of steric and electronic factors arising from its interaction with organotin(IV) species in the light of previous discussions on stereoelectronic effects [4]. The crystal structure determination of $[MeSnCl_2L^3]$ has permitted interesting comparisons with those of related complexes, as well as with the uncoordinated anion.

2. Results and discussion

The compounds of Table 1 were obtained by interaction of the potassium salt of the pyrazolylborate and Me_nSnCl_{4-n} in dichloromethane solution/suspension, following previously established procedures [4b,c]. However, separation of KCl was in this case exceedingly slow in comparison with other L, and yields are poorer. The complexes are also more air-sensitive, especially **1**, while **3** is prone to slow decomposition even when stored under N_2.

* Corresponding author.

SSDI 0022-328X(94)05003-T

Table 1
Yields, analyses, and physical properties of the compounds

	Compound [a]	Yield	Elemental Analysis (Found/Calcd.) (%)			M.W.	Λ [c]
			C	H	N		
	KL^3H_2O [b]	56	54.27	7.56	20.96		
			54.54	7.63	21.20		
1	$[SnCl_3L^3]$ [b]	64	38.56	5.10	14.21		4.9
			38.31	5.00	14.89		(1.0)
2	$[CH_3SnCl_2L^3]$ [b]	76	41.74	5.84	15.19	527 [d]	7.5
			41.96	5.74	15.45		(1.1)
3	$[(CH_3)_2SnClL^3]$ [b]	62	45.33	6.42	15.81	510 [d]	8.9
			45.89	6.55	16.05		(1.0)

[a] L^3 is hydridotris(3,4,5-trimethyl-1*H*-pyrazol-1-yl)borate $C_{18}H_{28}N_6B$. [b] It chars without melting [c] Specific conductivity ($ohm^{-1}cm^2mol^{-1}$) in acetone solution at room temperature and the molar concentration $\times 10^{-3}$ indicated in parentheses. [d] Monomer according to molecular-weight determination by osmometry in dichloromethane.

The complexes have been characterised by the analytical data (Table 1) and yields. As expected of neutral complexes in which the metal cation is encased in a hydrophobic shell, and like the analogues with L^0, L^1, and L^2, the compounds are monomers in non-donor solvents (dichloromethane) and non-electrolytes in acetone solution.

The IR spectra of the compounds (Table 2) exhibit the bands expected of pyrazole rings, weak C–H stretching vibration(s) at ca. 3150–3100 cm^{-1}, strong ring "breathing" vibrations at 1596–1583 cm^{-1}, and ca. 1570 cm^{-1}, and medium intensity ν(B–H) peaks around 2550 cm^{-1}, the frequency of which increases with the number of tin-bonded chlorine atoms. Others bands in the low frequency region are due to ν(Sn–C) and ν(Sn–Cl).

The ^1H (Table 3), ^{13}C, and ^{119}Sn (Table 4) NMR spectra support the proposed formulae. Two sets of signals are evident (except in **1**) in both ^1H-(2:1) and ^{13}C-spectra (one more intense than the other) for the pyrazole rings. This reflects the difference of one ring from the other two because the virtual C_{3v} symmetry of the anion is lost when tin-bonded substituents are not the same. Indeed, this confirms that octahedral

Table 2
IR data

Compound	Pyrazole C–H stretching	B–H	ring breathing	< 500	others
KL^3	3200 w, sh; 3156 w;	2430 m	1596 s	310 w	
	3094 w, sh		1570 s		
1	3150 w,	2568 m	1594 s	380 w	ν(Sn–Cl) 330 vs
	3102 w		1540		
2	3115 w, sh	2561 m	1596 w	350 w	ν(SN–Cl) 290 s, br
	3105 w		1560 m		
			1519 s		
3	3132 w, sh	2541 m	1583 s	350 w;	ν(Sn–Cl) 295 s, br
	3110 m		1568 m sh		
			1517 s		

Table 3
^1H NMR data [a]

No.	Compound	Solvent	5- or 4 or 3-H δ [b]			R-Sn, ^nJ(Sn–H)/Hz and notes	
	KL^3	$(CD_3)_2CO$	1.80	1.95	2.08		
1	$SnCl_3L^3$	$CDCl_3$	1.99	2.42	2.46		
			1.98	2.32	2.60		
2	$MeSnCl_2L^3$	$CDCl_3$	1.82	2.34	2.48	Me: 1.50	$^2J = 120$
			1.80	2.32	2.78		
3	Me_2SnClL^3	$CDCl_3$	1.98	2.25	2.55	Me: 0.99	
			1.82	2.27	2.35		

[a] In ppm from internal TMS. [b] The upper line signal has twice the intensity of that in the lower line.

Table 4
^{13}C and ^{119}Sn NMR data

No.	Compound	Solvent	C-3 δ [a,b]	C-5 δ	C-4 δ	Pz–CH_3 δ	R–Sn [a] and	^{119}Sn $-\delta$ [c]
	KL^3	$(CD_3)_2CO$	144.6	139.9	108.7	12.1 11.0 8.2		
1	$SnCl_3L^3$	$CDCl_3$	*	141.2	110.3	14.3 10.4 7.4		659
2	$MeSnCl_2L^3$	$CDCl_3$	148.0	142.1	112.9	12.1 10.8 7.7	Me: 26.0	514
			149.7	141.9	113.5	13.6 11.2 7.8		
3	Me_2SnClL^3	$CDCl_3$	147.5	142.0	111.5	12.7 10.5 7.3	Me: 19.1	365
			145.2	140.6	112.3	13.5 11.1 7.8		

[a] In ppm from Me_4Si, calibration from internal deuterium solvent lock. [b] The signals on the upper line are more intense than those on the lower line. [c] In ppm from external Me_4Sn. * not observed.

geometry is preserved in solution and furthermore rules out fluxionality around tin, which was found in some derivatives of L^0 at 25°C (but frozen at −30°C) [4a]. This also means that the sharp peak observed in ^{119}Sn-NMR spectra is due to a single species. The resonances of ring carbon atoms in the complexes are however always at higher positions than in KL^3 and follow the sequence $[Cl_3SnL^3] > [MeCl_2SnL^3] > [Me_2ClSnL^3]$, reflecting decreased flow of charge from the pz-rings to the the tin moiety as it becomes a poorer Lewis acid. The same trend is observable in the proton spectra.

2.1. Description of the molecular structures

Perspective drawings of **2** and KL^3 are shown in Figs. 1 and 2 together with the numbering scheme.

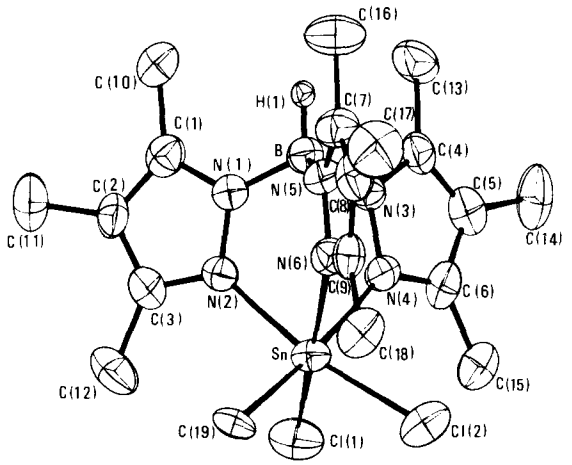

Fig. 1. Molecular structure of compound **2** and labelling scheme drawn with 50% thermal ellipsoids.

Crystallographic data are reported in Table 5, final atomic coordinates and equivalent isotropic thermal parameters with standard deviations are listed in Table 6, while selected interatomic distances and angles are reported in Table 7. The crystal structure of **2** consists of discrete molecules made of a $MeSnCl_2$ moiety complexed by $HB(3,4,5\text{-}Me_3Pz)_3$ (L^3). The tin atom is six-coordinate, being bonded to two chlorine atoms, one methyl carbon atom and three nitrogen atoms of the tridentate L^3. The coordination sphere is thus essentially octahedral. In **2** the Sn–N bond lengths are not significantly different and average 2.242(6) Å while the

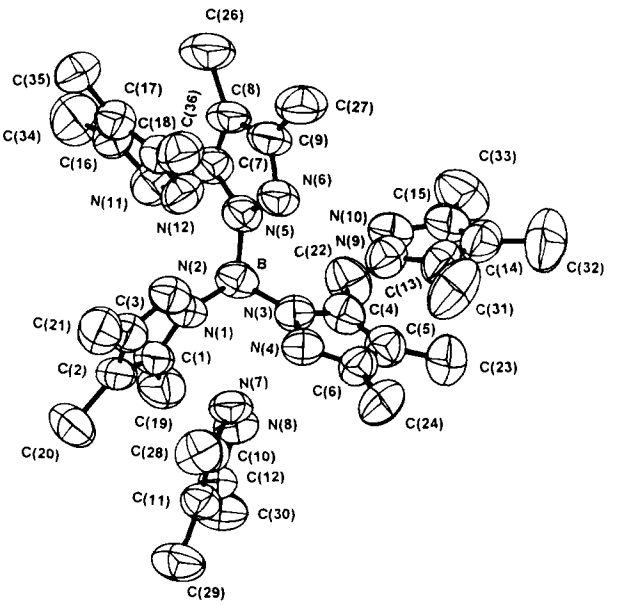

Fig. 2. Molecular structure of compound KL^3 and labelling scheme drawn with 50% thermal ellipsoids.

Table 5
Crystallographic data

Compound	2	KL^3 3PzH·0.5 EtzO
Formula	$C_{19}H_{31}BCl_2N_6Sn$	$C_{36}H_{58}BKN_{12}\cdot\frac{1}{2}C_4H_{10}O$
Fw	543.91	745.91
Crystal system	Monoclinic	Monoclinic
Space group	*C* 2/*c*	*C* 2/*c*
a (Å)	30.515(8)	20.845(19)
b (Å)	10.145(2)	21.267(8)
c (Å)	16.119(3)	20.409(8)
α, β, γ, (°)	90.00, 92.34(3), 90.00	90.00, 91.51(6), 90.00
V (Å^3)	4985.87	9044.39
Z	8	8
d_{calc}, g cm^{-3}	1.450	1.096
μ (cm^{-1})	12.62	13.37
F(000)	2208.0	3224.00
No. of measd reflcns	6538	6772
No. of unique reflcns	6030	6122
Obsd reflcns, $I > 3\sigma(I)$	3419	2501
Function minimized	$\Sigma w(F_o - F_c)^2$	
No. of params refined	262	471
a, *b* values in the weight Function:		
$w = 1.0/(a + F_0 + bF_0)$	43.2162 0.00321	12.056 0.01109
R [a]	0.053	0.062
R_w [a]	0.074	0.081
Goodness of fit, *s*	0.5	0.3

[a] $R = \Sigma||F_o| - |F_c||/\Sigma|F_o|$; $R_w = \{\Sigma w(|F_o| - |F_c|)^2/\Sigma w|F_o|^2\}^{1/2}$.
[b] $s = \{\Sigma w(|F_o| - |F_c|)^2/(N_{refl} - N_{param})\}^{1/2}$.

two Sn–Cl bonds differ by ca. 8.7 σ, as found in $[PhSnCl_2L^1]$ (9.0 σ) [4c] or $[RSnCl_2L^0]$ (14.5σ) [11]. There is no obvious explanation for this difference.

The salt KL^3 crystallises with three free 3,4,5-trimethylpyrazole (pz) molecules and one half molecule of diethyl ether.

The geometry of the Sn and B bonded pyrazole ring (A) in **2** compares quite well with those in KL^3 (B) or free (C). The average values of bond distances N–N one 1.366(9) (A), 1.38(1) (B) and 1.39(1) (C) N–C is 1.35(1) (A), (B), (C), C–C is 1.38(1) Å (A), (B) and (C) and the angles at $N_1 \simeq C_3$ are 109.7(7) (A), 110.7(7) (B) and 110.9(8) (C), $N_2 \simeq C_4$ are 106.3(7) (A), 105.4(7) (B), and 105.0(8) (C) and at C5 are 108.1(7) (A), 107.9(8) (B) and 108.2(9)° (C) (see Fig. 3 for the nomenclature). These are consistent with previously proposed rules [7] and with that determined elsewhere [8], but at variance with the case of $[PhSnCl_2L^1]$ [4c]. The five atoms of each pyrazole are planar within experimental error.

The boron atom has a tetrahedral configuration, the N–B–N angles ranging from 108.6(6) to 110.0(6) in **2** and 109.2(6) to 110.9(6) in KL^3. The angles B–N–N are smaller then the B–N–C angles, the differences in **2** being greater than those in KL^3. The N–B–N–N torsion angles average 60.0° in **2**, while the corresponding values in KL^3 are in the range 26(1)–94.3(8)°.

Distances and angles around the K atom in KL^3 are reported in Table 8. From these values it appears possible to identify six N–K interactions. The plane A defined by N(2), N(4), and N(6), and the plane B defined by N(7), N(9), and N(12), are almost parallel (the dihedral angle A∧B is 1.2°). The K atom is located between these planes and it lies 2.24 Å from plane A and 0.43 Å from plane B. The arrangement around K^+ can be described as a distorted trigonal prism with the K pushed to one end (Fig. 4). If we define M1 as the centre of N atoms in the plane A and M2 as the centre of N atoms in the plane B, the angle M1–K–M2 is 170.0°. All the intermolecular contacts in the crystals of **2** and KL^3 are longer than the sum of the Van der Waals radii [9]. The shortest Cl....C intermolecular contact is Cl(1)....C(12) 3.64(1) Å in compound **2**.

From Table 9, and from comparison within First-Row transition metal bis(trispyrazolylborates)$[M(L)_2]$ (L = L^0, L^1 or L^2) [6c,10], it is clear that the presence of a 3-Me in the ligand pz-rings lengthens the Sn–N bond and slightly increases the bite angles. The latter are greatest in L^3, but the corresponding increase in bond length may not be entirely comparable with the L^1 case since a phenyl group has greater steric demand than a methyl. The reason why this happens can be explained only in terms of steric crowding of three 3-Me groups in the equatorial belt together with the three other substituents bonded to octahedral tin (Me, Cl, Cl in **2**).

The two structures recorded allow interesting, internally consistent comparisons between three types of pyrazole moiety. While bond lengths do not show any significant variation, the bond angles α, β, and γ (see Fig. 5) show significant trends. As N-2 is bonded to Sn (and so closing the cage) the angle α shrinks by 2.2°. In KL^3 three 5-Me groups rotate backwards in order to relieve steric congestion at the boron ($\beta_B - \beta_C = 2.4°$) while the γ angles remain almost the same ($\gamma_B - \gamma_C = 0.5°$). The three 3-Me ones in **2** also experience steric hindrance in that, although the Sn–N bond is longer than the N–B (Table 9), they compete for space with three other substituents on tin ($\gamma_A - \gamma_B = 2.7°$) in the resulting cog-wheel arrangement. This does not happen in KL^3 since K^+ causes only weak electrostatic

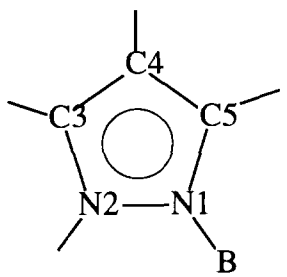

Fig. 3. Atomic numbering used for the pyrazole ring.

Table 6
Atomic coordinates and isotropic thermal parameters, B_{eq} (Å^2) of the non-hydrogen atoms in **2** and KL^3 (Esd in values parentheses) [a]

Atom	x	y	z	B_{eq}
Compound **2**				
Sn(1)	0.84904(2)	0.07647(5)	0.04298(3)	3.46(1)
Cl(1)	0.8338(1)	0.2663(2)	−0.0450(2)	5.7(1)
Cl(2)	0.8960(1)	0.1984(2)	0.1432(1)	5.6(1)
B(1)	0.8832(3)	−0.2003(8)	−0.0441(5)	3.5(2)
N(1)	0.8370(2)	−0.1662(6)	−0.0781(4)	3.6(2)
N(2)	0.8168(2)	−0.0556(6)	−0.0527(4)	3.7(2)
N(3)	0.9142(2)	−0.0855(6)	−0.0640(4)	3.6(1)
N(4)	0.9079(2)	0.0381(6)	−0.0319(4)	3.4(2)
N(5)	0.8830(2)	−0.2182(6)	0.0511(4)	3.4(1)
N(6)	0.8707(2)	−0.1157(6)	0.1007(4)	3.4(1)
C(1)	0.8100(3)	−0.2344(8)	−0.1304(5)	4.1(2)
C(2)	0.7712(3)	−0.1642(8)	−0.1398(5)	4.0(2)
C(3)	0.7759(3)	−0.0558(8)	−0.0906(6)	4.4(2)
C(4)	0.9523(2)	−0.0870(9)	−0.1033(4)	3.6(2)
C(5)	0.9704(3)	0.0375(9)	−0.0992(5)	4.2(2)
C(6)	0.9423(3)	0.1122(8)	−0.0537(5)	4.1(2)
C(7)	0.8956(3)	−0.3209(7)	0.0981(5)	4.1(2)
C(8)	0.8917(3)	−0.2862(8)	0.1802(5)	4.2(2)
C(9)	0.8763(2)	−0.1581(8)	0.1795(5)	3.6(2)
C(10)	0.8227(3)	−0.360(1)	−0.1708(7)	5.6(3)
C(11)	0.7305(3)	−0.204(1)	−0.1937(7)	6.3(3)
C(12)	0.7435(4)	0.053(1)	−0.0784(8)	7.1(4)
C(13)	0.9676(3)	−0.207(1)	−0.1482(6)	5.2(3)
C(14)	1.0130(3)	0.083(1)	−0.1334(6)	6.2(3)
C(15)	0.9475(3)	0.2554(9)	−0.0321(6)	4.8(2)
C(16)	0.9109(4)	−0.4480(8)	0.0624(7)	6.4(3)
C(17)	0.9026(4)	−0.369(1)	0.2560(7)	6.7(3)
C(18)	0.8657(3)	−0.075(1)	0.2538(5)	5.1(2)
C(19)	0.7891(2)	0.0865(7)	0.1189(4)	3.6(2)
Compound KL^3				
K(1)	0.2856(1)	0.0512(1)	0.2153(1)	6.8(1)
O(1)	1.0000	0.4143(9)	0.2500	19.1(5)
B(1)	0.1754(4)	0.2005(5)	0.2233(4)	6.5(3)
N(1)	0.1624(3)	0.1566(3)	0.2814(3)	6.2(2)
N(2)	0.1692(3)	0.0925(4)	0.2765(3)	7.0(2)
N(3)	0.2462(3)	0.2219(3)	0.2243(3)	6.2(2)
N(4)	0.2946(3)	0.1856(3)	0.2537(3)	6.3(2)
N(5)	0.1595(3)	0.1648(3)	0.1578(3)	6.4(2)
N(6)	0.2057(3)	0.1338(3)	0.1244(3)	7.0(2)
N(7)	0.3275(3)	0.0460(4)	0.3542(3)	7.1(2)
N(8)	0.3116(3)	0.1072(4)	0.3682(3)	7.1(2)
N(9)	0.3766(4)	0.0990(3)	0.1244(3)	7.5(2)
N(10)	0.3412(4)	0.1475(4)	0.0961(4)	7.7(2)
N(11)	0.1362(4)	−0.0072(4)	0.1802(4)	8.5(3)
N(12)	0.1919(3)	−0.0400(4)	0.1760(3)	7.6(2)
C(1)	0.1471(4)	0.1723(5)	0.3437(4)	6.7(3)
C(2)	0.1458(4)	0.1174(5)	0.3803(4)	7.1(3)
C(3)	0.1585(4)	0.0695(5)	0.3363(5)	7.2(3)
C(4)	0.2728(5)	0.2732(4)	0.1970(4)	6.8(3)
C(5)	0.3374(5)	0.2720(5)	0.2065(4)	7.4(3)
C(6)	0.3492(4)	0.2164(5)	0.2417(4)	7.0(3)
C(7)	0.1014(4)	0.1582(4)	0.1279(4)	7.5(3)
C(8)	0.1105(4)	0.1207(5)	0.0740(4)	7.9(3)
C(9)	0.1746(4)	0.1074(4)	0.0730(4)	7.4(3)
C(10)	0.3460(4)	0.0216(4)	0.4116(4)	6.7(3)
C(11)	0.3423(4)	0.0657(4)	0.4620(4)	6.8(3)
C(12)	0.3201(4)	0.1202(4)	0.4324(4)	6.8(3)
C(13)	0.4348(4)	0.1074(5)	0.1004(5)	7.7(3)
C(14)	0.4376(5)	0.1588(6)	0.0576(5)	8.4(4)
C(15)	0.3773(6)	0.1835(5)	0.0568(5)	8.1(3)
C(16)	0.0844(4)	−0.0421(6)	0.1597(4)	8.5(4)
C(17)	0.1072(6)	−0.0996(5)	0.1425(4)	8.2(3)
C(18)	0.1731(5)	−0.0965(5)	0.1525(4)	7.2(3)
C(19)	0.1375(4)	0.2389(4)	0.3649(4)	8.9(3)
C(20)	0.1333(5)	0.1103(5)	0.4528(4)	10.4(4)
C(21)	0.1647(4)	0.0001(5)	0.3504(4)	8.9(3)
C(22)	0.2323(5)	0.3220(4)	0.1621(4)	9.0(3)
C(23)	0.3867(5)	0.3190(5)	0.1860(5)	10.2(4)
C(24)	0.4116(4)	0.1886(4)	0.2649(5)	9.0(3)
C(25)	0.0414(4)	0.1861(6)	0.1543(5)	11.4(4)
C(26)	0.0602(5)	0.0992(6)	0.0227(4)	12.2(5)
C(27)	0.2104(5)	0.0672(5)	0.0251(4)	10.5(4)
C(28)	0.3686(4)	−0.0460(4)	0.4176(5)	8.6(3)
C(29)	0.3604(5)	0.0580(5)	0.5337(4)	9.9(4)
C(30)	0.3065(5)	0.1847(4)	0.4574(4)	9.2(3)
C(31)	0.4881(4)	0.0625(5)	0.1210(6)	11.9(5)
C(32)	0.4948(5)	0.1825(5)	0.0223(6)	12.6(5)
C(33)	0.3462(6)	0.2390(6)	0.0208(5)	11.8(4)
C(34)	0.0177(5)	−0.0141(6)	0.1604(5)	12.4(5)
C(35)	0.0675(5)	−0.1549(5)	0.1182(5)	11.0(4)
C(36)	0.2219(5)	−0.1474(4)	0.1414(5)	9.0(3)
C(37)	0.9491(9)	0.3802(9)	0.234(1)	26(1)
C(38)	0.8951(7)	0.4234(8)	0.2215(7)	16.4(7)

[a] $B_{eq} = (4/3)\Sigma_i\Sigma_j\beta_{ij}a_ia_j$.

interactions with the N-2 atoms and does not require a closer approach to the latter, so avoiding steric crowding of 3-Me groups. The effect of the 4-Me groups can be seen by comparing the present γ value with that in [$PhCl_2SnL^1$], $\gamma_{L^1}-\gamma_{L^3} = 2.0°$ [4c]. The higher value in the case of L^1 may be due to the absence of a 4-Me allowing a greater distortion of the 3-Me.

Considering $\delta(^{119}Sn)$ as a function of the number of tin-bonded Me groups n, parameterized by the variation of the ligand, one obtains the plot of Fig. 6. As shown, the δ values for the four series [Me_nCl_{4-n-1}-SnL] ($0 \leq n \leq 2$) are almost parallel linear functions of n [2–4c].

This is a further confirmation of the absence of sudden changes in solution structure upon changing the ligands. The ligands bearing Me-substituted pyrazole rings cause higher negative displacements than the parent L^0. Differences between the lines relating to L^1, L^2, or L^3 are very small but, for each n the sequence of lines is the same as the order of methyl substitution. The only major change in ^{119}Sn δ it occurs in passing from (unsubstituted) L^0 to the other (Me-substituted) ligands. Comparison of the above data with the Sn–N bond length leads to the conclusion that steric hindrance is an important factor if there is 3-Me substitutuent, while Me groups in other positions play only a minor role.

3. Experimental details

Concentration was always carried out in vacuo (water aspirator). The samples were dried in vacuo to con-

Table 7
Selected bond distances (Å) and bond angles (°) for **2** and $KL^3 \cdot 3PzH \cdot 0.5Et_2O$ with esd values in parentheses

Compound **2**			
Bond distances			
Sn(1)–Cl(1)	2.425(3)	N(6)–C(9)	1.35(1)
Sn(1)–Cl(2)	2.451(3)	C(1)–C(2)	1.38(1)
Sn(1)–N(2)	2.240(6)	C(1)–C(10)	1.49(1)
Sn(1)–N(4)	2.239(6)	C(2)–C(3)	1.36(1)
Sn(1)–N(6)	2.247(6)	C(2)–C(11)	1.54(1)
Sn(1)–C(19)	2.244(7)	C(3)–C(12)	1.50(1)
B(1)–N(1)	1.53(1)	C(4)–C(5)	1.38(1)
B(1)–N(3)	1.54(1)	C(4)–C(13)	1.50(1)
B(1)–N(5)	1.55(1)	C(5)–C(6)	1.38(1)
N(1)–N(2)	1.352(9)	C(5)–C(14)	1.51(1)
N(1)–C(1)	1.35(1)	C(6)–C(15)	1.50(1)
N(2)–C(3)	1.37(1)	C(7)–C(8)	1.38(1)
N(3)–N(4)	1.373(9)	C(7)–C(16)	1.49(1)
N(3)–C(4)	1.347(9)	C(8)–C(9)	1.38(1)
N(4)–C(6)	1.35(1)	C(8)–C(17)	1.51(1)
N(5)–N(6)	1.373(8)	C(9)–C(18)	1.51(1)
N(5)–C(7)	1.33(1)		
Bond angles			
Cl(2)–Sn(1)–Cl(1)	94.45(9)	C(4)–N(3)–N(4)	109.0(6)
N(2)–Sn(1)–Cl(1)	90.2(2)	N(6)–N(5)–B(1)	120.0(6)
N(2)–Sn(1)–Cl(2)	169.9(2)	C(7)–N(5)–B(1)	130.0(6)
N(4)–Sn(1)–Cl(1)	87.8(2)	C(7)–N(5)–N(6)	110.0(6)
N(4)–Sn(1)–Cl(2)	89.0(2)	C(2)–C(1)–N(1)	107.6(7)
N(4)–Sn(1)–N(2)	82.2(2)	C(10)–C(1)–N(1)	123.4(8)
N(6)–Sn(1)–Cl(1)	167.6(2)	C(10)–C(1)–C(2)	129.0(8)
N(6)–Sn(1)–Cl(2)	90.6(2)	C(3)–C(2)–C(1)	106.4(7)
N(6)–Sn(1)–N(2)	83.1(2)	C(11)–C(2)–C(1)	126.3(8)
N(6)–Sn(1)–N(4)	81.0(2)	C(11)–C(2)–C(3)	127.2(8)
C(19)–Sn(1)–Cl(1)	98.1(2)	C(2)–C(3)–N(2)	109.5(7)
C(19)–Sn(1)–Cl(2)	94.8(2)	C(12)–C(3)–N(2)	122.3(8)
C(19)–Sn(1)–N(2)	93.3(3)	C(12)–C(3)–C(2)	128.1(9)
C(19)–Sn(1)–N(4)	172.6(2)	C(5)–C(4)–N(3)	108.5(7)
C(19)–Sn(1)–N(6)	92.6(2)	C(13)–C(4)–N(3)	121.9(7)
N(1)–N(2)–Sn(1)	120.8(5)	C(13)–C(4)–C(5)	129.4(7)
C(3)–N(2)–Sn(1)	132.5(5)	C(6)–C(5)–C(4)	105.9(7)
C(3)–N(2)–N(1)	106.4(6)	C(14–C(5)–C(4)	127.9(8)
N(3)–N(4)–Sn(1)	119.4(4)	C(14)–C(5)–C(6)	126.2(9)
C(6)–N(4)–Sn(1)	133.8(5)	C(5)–C(6)–N(4)	109.8(7)
C(6)–N(4)–N(3)	106.8(6)	C(15)–C(6)–N(4)	123.7(7)
N(5)–N(6)–Sn(1)	120.0(4)	C(15)–C(6)–C(5)	126.4(8)
C(9)–N(6)–Sn(1)	133.8(5)	C(8)–C(7)–N(5)	108.1(7)
C(9)–N(6)–N(5)	106.2(6)	C(16)–C(7)–N(5)	122.9(8)
N(3)–B(1)–N(1)	108.6(6)	C(16)–C(7)–C(8)	129.0(8)
N(5)–B(1)–N(1)	110.0(6)	C(9)–C(8)–C(7)	105.9(7)
N(5)–B(1)–N(3)	108.8(6)	C(17)–C(8)–C(7)	127.5(8)
N(2)–N(1)–B(1)	120.2(6)	C(17)–C(8)–C(9)	126.5(8)
C(1)–N(1)–B(1)	129.7(7)	C(8)–C(9)–N(6)	109.8(7)
C(1)–N(1)–N(2)	110.0(6)	C(18)–C(9)–N(6)	123.3(7)
N(4)–N(3)–B(1)	120.9(6)	C(18)–C(9)–C(8)	126.9(7)
C(4)–N(3)–B(1)	129.7(7)		
Compound KL^3			
Bond distances			
O(1)–C(37)	1.31(2)	C(4)–C(5)	1.35(1)
B(1)–N(1)	1.53(1)	C(4)–C(22)	1.50(1)
B(1)–N(3)	1.54(1)	C(5)–C(6)	1.40(1)
B(1)–N(5)	1.56(1)	C(5)–C(23)	1.50(1)
N(1)–N(2)	1.37(1)	C(6)–C(24)	1.49(1)
N(1)–C(1)	1.35(1)	C(7)–C(8)	1.37(1)
N(2)–C(3)	1.33(1)	C(7)–C(25)	1.49(1)
N(3)–N(4)	1.391(8)	C(8)–C(9)	1.36(1)
N(3)–C(4)	1.34(1)	C(8)–C(26)	1.53(1)
N(4)–C(6)	1.34(1)	C(9)–C(27)	1.51(1)

Table 7 (continued)

N(5)–N(6)	1.363(8)	C(10)–C(11)	1.39(1)
N(5)–C(7)	1.347(9)	C(10)–C(28)	1.51(1)
N(6)–C(9)	1.34(1)	C(11)–C(12)	1.38(1)
N(7)–N(8)	1.37(1)	C(11)–C(29)	1.51(1)
N(7)–C(10)	1.33(1)	C(12)–C(30)	1.49(1)
N(8)–C(12)	1.34(1)	C(13)–C(14)	1.40(2)
N(9)–N(10)	1.38(1)	C(13)–C(31)	1.51(1)
N(9)–C(13)	1.33(1)	C(14)–C(15)	1.36(1)
N(10)–C(15)	1.35(1)	C(14)–C(32)	1.49(1)
N(11)–N(12)	1.35(1)	C(15)–C(33)	1.52(1)
N(11)–C(16)	1.36(1)	C(16)–C(17)	1.36(1)
N(12)–C(18)	1.34(1)	C(16)–C(34)	1.51(1)
C(1)–C(2)	1.38(1)	C(17)–C(18)	1.38(1)
C(1)–C(19)	1.49(1)	C(17)–C(35)	1.51(1)
C(2)–C(3)	1.38(1)	C(18)–C(36)	1.50(1)
C(2)–C(20)	1.51(1)	C(37)–C(38)	1.47(2)
C(3)–C(21)	1.50(1)		
Bond angles			
N(3)–B(1)–N(1)	110.8(6)	C(24–C(6)–C(5)	129.4(8)
N(5)–B(1)–N(1)	109.1(6)	C(8)–C(7)–N(5)	106.3(6)
N(5)–B(1)–N(3)	109.7(5)	C(25)–C(7)–N(5)	122.9(7)
N(2)–N(1)–B(1)	121.5(6)	C(25)–C(7)–C(8)	130.5(7)
C(1)–N(1)–B(1)	128.5(7)	C(9)–C(8)–C(7)	106.6(7)
C(1)–N(1)–N(2)	109.7(6)	C(26)–C(8)–C(7)	127.9(8)
C(3)–N(2)–N(1)	105.9(6)	C(26)–C(8)–C(9)	125.4(7)
N(4)–N(3)–B(1)	121.4(6)	C(8)–C(9)–N(6)	110.7(7)
C(4)–N(3)–B(1)	129.4(6)	C(27)–C(9)–N(6)	120.3(7)
C(4)–N(3)–N(4)	109.0(6)	C(27)–C(9)–C(8)	128.8(7)
C(6)–N(4)–N(3)	104.9(6)	C(11)–C(10)–N(7)	111.4(7)
N(6)–N(5)–B(1)	121.5(5)	C(28)–C(10)–N(7)	121.6(7)
C(7)–N(5)–B(1)	127.2(6)	C(28)–C(10)–C(11)	126.9(7)
C(7)–N(5)–N(6)	111.2(6)	C(12)–C(11)–C(10)	105.4(7)
C(9)–N(6)–N(5)	105.0(6)	C(29)–C(11)–C(10)	128.5(8)
C(10)–N(7)–N(8)	104.6(6)	C(29)–C(11)–C(12)	126.0(7)
C(12)–N(8)–N(7)	111.7(6)	C(11)–C(12)–N(8)	106.6(7)
C(13)–N(9)–N(10)	103.1(7)	C(30)–C(12)–N(8)	119.9(7)
C(15)–N(10)–N(9)	111.7(7)	C(30)–C(12)–C(11)	133.3(7)
C(16)–N(11)–N(12)	111.8(7)	C(14)–C(13)–N(9)	112.7(8)
C(18)–N(12)–N(11)	103.7(6)	C(31–C(13)–N(9)	118.8(8)
C(2)–C(1)–N(1)	107.8(8)	C(31)–C(13)–C(14)	128.4(8)
C(19)–C(1)–N(1)	122.6(8)	C(15)–C(14)–C(13)	104.8(8)
C(19)–C(1)–C(2)	129.4(7)	C(32)–C(14)–C(13)	127.5(9)
C(3)–C(2)–C(1)	105.1(7)	C(32)–C(14)–C(15)	127 (1)
C(20)–C(2)–C(1)	128.1(9)	C(14)–C(15)–N(10)	107.5(9)
C(20)–C(2)–C(3)	126.7(9)	C(33)–C(15)–N(10)	119.1(9)
C(2)–C(3)–N(2)	111.2(8)	C(33)–C(15)–C(14)	133.2(9)
C(21)–C(3)–N(2)	121.0(8)	C(17)–C(16)–N(11)	106.6(8)
C(21)–C(3)–C(2)	127.6(8)	C(34)–C(16)–N(11)	120 (1)
C(5)–C(4)–N(3)	110.0(7)	C(34)–C(16)–C(17)	133 (1)
C(22)–C(4)–N(3)	121.3(8)	C(18)–C(17)–C(16)	105.7(9)
C(22)–C(4)–C(5)	128.5(8)	C(35)–C(17)–C(16)	126.1(9)
C(6)–C(5)–C(4)	104.4(7)	C(35)–C(17)–C(18)	128.0(9)
C(23)–C(5)–C(4)	129.2(8)	C(17)–C(18)–N(12)	111.9(8)
C(23)–C(5)–C(6)	126.2(8)	C(36)–C(18)–N(12)	120.1(8)
C(5)–C(6)–N(4)	111.5(7)	C(36)–C(18)–C(17)	127.9(9)
C(24)–C(6)–N(4)	119.0(7)	C(38)–C(37)–O(1)	107 (1)

stant weight (20°C, ca. 0.1 torr). Carbon, hydrogen, and nitrogen analyses were carried out in our Department; molecular weight determinations were performed at Pascher Mikroanalytisches Laboratorium, Remagen, Germany. IR spectra were recorded from 4000 to 250 cm^{-1} on a Perkin-Elmer 2000 FTIR instrument. ^1H-,

Table 8
Distances (Å) and angles (°) around the K cation in $KL^3 \cdot 3PzH \cdot 0.5Et_2O$ with e.s.d. values in parentheses

Distances					
B(1)	3.923(9)				
N(1)	3.691(6)	N(5)	3.736(6)	N(9)	2.872(7)
N(2)	2.894(6)	N(6)	3.022(6)	N(10)	3.404(7)
N(3)	3.727(6)	N(7)	2.946(6)	N(11)	3.411(8)
N(4)	2.967(6)	N(8)	3.371(6)	N(12)	2.852(7)
Angles					
N(2)–K–N(4)	69.0(1)		N(4)–K–N(12)	140.0(2)	
N(2)–K–N(6)	68.5(1)		N(6)–K–N(7)	139.1(1)	
N(2)–K–N(7)	80.0(1)		N(6)–K–N(9)	76.1(1)	
N(2)–K–N(9)	138.3(2)		N(6)–K–N(12)	82.0(1)	
N(2)–K–N(12)	75.6(2)		N(7)–K–N(9)	116.7(2)	
N(4)–K–N(6)	68.4(1)		N(7)–K–N(12)	115.3(2)	
N(4)–K–N(7)	76.5(1)		N(9)–K–N(12)	121.1(2)	
N(4)–K–N(9)	78.0(1)				

Table 9
Comparison of structural factors for related organotin(IV) compounds $R_nSnX_{4-n-1} \cdot L$

L	R-group	n	X-group	Mean Sn–N distance (Å)	Mean N–Sn–N bite angles (°)	Ref.
L^3	Me	1	Cl	2.242	82.0	[a]
L^1	Ph	1	Cl	2.249	81.6	[4c]
L^0	CH_2R [b]	1	Cl	2.218	80.3	[11]
L^0	CH_2R [b]	1	NCS	2.218	81.1	[11]
L^0	Me	3	–	2.388	74.8	[12]

[a] Present paper; [b] R = CH_2COOMe.

^{13}C- and ^{119}Sn-NMR spectra were recorded on a Varian VX-300 spectrometer operating at room temperature (300 MHz for ^1H, 75 MHz for ^{13}C and 111.9 MHz for ^{119}Sn). The electrical resistance of acetone solutions was measured with a Crison CDTM 522 conductimeter at room temperature.

3.1. 3,4,5-trimethylpyrazole

The pyrazole was prepared from 3-methyl-2,4-pentanedione and $N_2H_4 \cdot H_2O$ in EtOH essentially following the procedure in Ref. [6]. The recrystallised product (hexane) was obtained in 63% yield and melted at 136.5–137.5°C (Lit. 136–137°C [13]).

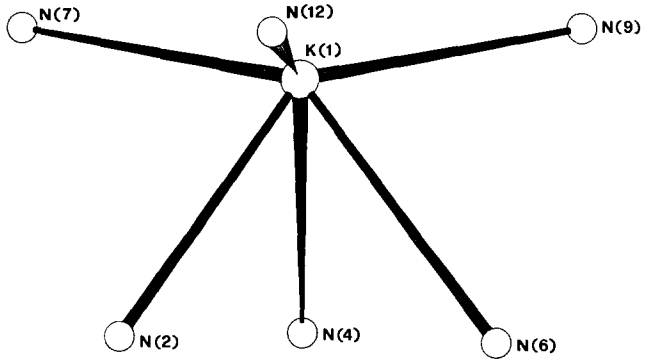

Fig. 4. Interactions around the K atom: the Newman projection along M1–M2 giving the orientation of the N atoms belonging to the ligand with respect to the N atoms belonging to the free pyrazoles.

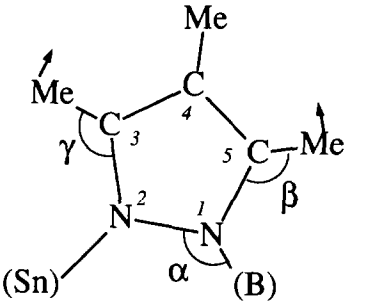

	A (Sn-μ-pz-B)	B (pz-B)	C (pz-H)
α / °	108.6	110.8	-
β / °	122.7	122.3	119.9
γ / °	123.1	120.4	119.9

Fig. 5. Selected angles in the reported crystal structures.2e

3.2. Potassium hydridotris(3,4,5-trimethyl-1H-pyrazol-1-yl)borate (KL^3)

A mixture of 22.03 g (0.2 mol) of 3,4,5-trimethylpyrazole and 2.7 g (0.05 mol) of potassium borohydride was heated with stirring in a 120 ml flask attached through an air condenser connected to a gas meter. When about ~1.5 dm^3 of dihydrogen had been evolved, the oil bath was replaced by a heating mantle, and the temperature was raised gradually to 180°C within 3 h, and then held there for 36–48 h until a total

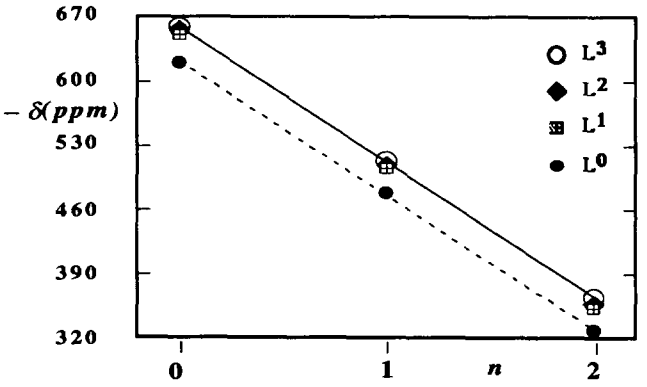

$-\delta(L^3) = 659.7 - 147.0\ n\ (r = 0.99997);$
$-\delta(L^2) = 657.0 - 149.3\ n\ (r = 0.99996);$
$-\delta(L^1) = 652.3 - 179.0\ n\ (r = 0.99988);$
$-\delta(L^0) = 621.8 - 145.9\ n\ (r = 0.99989);$

Fig. 6. Correlations between ^{119}Sn chemical shift for $Me_nCl_{4-n-1}Sn \cdot L$ ($L = L^0 - L^3$; $0 \le n \le 2$) and the number of tin-bonded methyl groups. L^1 and L^2 lines are not drawn, for clarity.

of 3.76 dm^3 (0.15 mol) of dihydrogen had been evolved. The melt was poured slowly into 70 ml of stirred hot xylene. The resulting mixture was stirred for 3–5 min and then filtered hot.

The solid was washed in heptane/diethyl ether (4:1 v/v) and air-dried yielding ~23 g (60%), and recrystallised from acetone-dichloromethane.

From recombined xylene/heptane/diethyl ether washings, colourless crystals of cubic shape separated after ca. one week. Elemental analysis C = 60.88, H = 8.60, N = 22.12 (Calcd. for $C_{36}H_{58}BKN_{12} \cdot \frac{1}{2}C_4H_{10}O$: C = 61.19, H = 8.51, N = 22.53%. One of these crystals was selected for X-ray structure determination.

3.3. *[Hydridotris(3,4,5-trimethyl-1H-pyrazol-1-yl)borate]dichloromethyltin(IV)* **2**

A solution of methyltrichlorotin(IV) (240 mg, 1 mmol) in dichloromethane (30 ml) was added to a stirred solution/suspension of potassium hydridotris (3,4,5-trimethyl-1*H*-pyrazol-1-yl)borate (378 mg, 1 mmol) in the same solvent (30 ml). After some hours, the filtered solution was evaporated to dryness, the residue washed with petroleum ether, and recrystallised from dichloromethane-diethyl ether. Suitable crystals of compound **2** were obtained by slow evaporation of a dichloromethane-acetonitrile solution at subambient temperature.

Compound **3** were obtained similarly. Compound **1** was recrystallised from dichloromethane/heptane.

3.4. *X-ray crystallographic analysis*

Crystal and experimental data are summarised in Table 5. A crystal of $C_{19}H_{31}BCl_2N_6Sn$ (compound **2**) obtained from a solution of CH_2Cl_2/MeCN, was mounted on a CS automatic four-circle diffractometer equipped with a Huber goniometer [14] using graphite monochromatised Mo-Kα radiation (λ = 0.71069 Å). The cell parameters were refined by least squares from the angular positions of 15 reflections in the range $8 < 2\theta < 22°$. The data were measured at room temperature for $3.0 < 2\theta < 60°$ from a crystal of approximate dimension of 0.44 × 0.38 × 0.20 mm, using $\theta/2\theta$ scan technique. The scan rate was automatically chosen according to the peak intensity in the range 3.0–30.0° min^{-1} and background counts were taken with stationary crystal at each end of the scan and total background time to scan time ratio of 0.5. A crystal of $C_{36}H_{58}BKN_{12} \cdot \frac{1}{2}C_4H_{10}O$ ($KL^3 \cdot 3Hpz \cdot \frac{1}{2}Et_2O$), obtained from a solution of xylene/*n*-C_7H_{16}/Et_2O, was mounted on a Siemens R3m/V automatic four-circle diffractometer using graphite monochromatized Cu-Kα radiation (λ = 1.54184 Å). The cell parameters were refined by least squares from the angular positions of 19 reflections in the range $8 < 2\theta < 29°$. The data were measured at room temperature for $3.0 < 2\theta < 115°$ from a crystal with approximate dimensions 0.5 × 0.5 × 0.25 mm, using the $\theta/2\theta$ scan technique. The scan rate was automatically chosen according to the peak intensity in the range 3.0–14.6° min^{-1} and background counts were taken with stationary crystal at each end of the scan and total background time to scan time ratio of 0.5.

The data for compounds **2** and KL^3 were processed [15] to yield values of I and $\sigma(I)$. The intensities of three standard reflections, measured every 97 reflections throughout the data collections, decayed by about 50.0% and 11.0% for **2** and KL^3, respectively. The values of I and $\sigma(I)$ were corrected for Lorentz and polarization effects and for decay and (only for **2**) an empirical absorption correction was done using method of Walker and Stuart [16] and the program written by Ugozzoli [17]. A total of 3419 and 2501 independent reflections having $I > 3\sigma(I)$ were used in all subsequent calculations for **2** and KL^3, respectively.

For **2** the tin atom coordinates were found from a Patterson map while for KL^3 an initial structural model was obtained by direct methods. In both cases the remaining atoms were located by successive structure factor calculations and Fourier maps. All non-hydrogen atoms were refined by full-matrix least squares methods with anisotropic thermal parameters. The hydrogen atoms were idealised (sp^3C–H = 1.08 Å, and sp^2C–H = 1.05 Å) [18]. Each H atom was assigned the equivalent isotropic temperature factor of the parent C atom and allowed to ride on it. The final difference Fourier map, with a root-mean-square deviation of electron density of 0.11 and 0.04 e $Å^{-3}$, showed no significant features. Atomic scattering factors were taken from [19]. Calculations were performed on the DEC 3500 AXP of Istituto di Strutturistica Chimica CNR, using the SIR CAOS [20] and SIR92 [21] structure determination packages.

Supplementary material available

Tables of observed and calculated structure factors are available from the authors. All other structural data (anisotropic thermal parameters for non-H atoms, hydrogen atoms parameters, atomic coordinaties, etc.) are available from the Cambridge Crystallographic Data Centre.

Acknowledgements

Financial support from the Consiglio Nazionale delle Ricerche (Rome), and from MURST is gratefully acknowledged. We thank Clara Marciante for technical assistance in the X-ray diffraction measurements.

References and notes

[1] (a) S. Trofimenko, *Chem. Rev., 93* (1993) 943; (b) *Progr. Inorg. Chem., 34* (1986) 115; (c) S. Trofimenko, *Top. Curr. Chem., 131* (1986) 1; (d) *Chem. Rev., 72* (1972) 497.

[2] (a) A.H. Cowley, R.L. Geerts, C.M. Nunn and C.J. Carrano, *J. Organomet. Chem., 341* (1988) C27; (b) D.L. Reger, S.J. Knox, M.F. Huff, A.L. Rheingold and B.S. Haggerty, *Inorg. Chem., 30* (1991) 1754; (c) M.N. Hansen, K. Niedenzu, J. Serwatowska and K.R. Woodrum, *Inorg. Chem., 30* (1991) 866; (d) S.K. Lee and B.N. Nicholson, *J. Organomet. Chem., 309* (1986) 257; (e) K. Niedenzu, H. Nöth, J. Serwatowska and J. Serwatowski, *Inorg. Chem., 30* (1991) 3249.

[3] (a) G. Gioia Lobbia, F. Bonati, P. Cecchi and C. Pettinari, *Gazz. Chim. Ital., 121* (1991) 355; (b) G. Gioia Lobbia, P. Cecchi, F. Bonati and G. Rafaiani, *Synth. React. Inorg. Met.-Org. Chem., 22* (1992) 775; (c) G. Gioia Lobbia, P. Cecchi, S. Bartolini, C. Pettinari and A. Cingolani, *Gazz. Chim. Ital., 123* (1993) 641.

[4] (a) G. Gioia Lobbia, F. Bonati, P. Cecchi, A. Cingolani and A. Lorenzotti, *J. Organomet. Chem., 378* (1989) 139; (b) G. Gioia Lobbia, F. Bonati, P. Cecchi, A. Lorenzotti and C. Pettinari, *J. Organomet. Chem., 403* (1991) 317; (c) G. Gioia Lobbia, S. Calogero, B. Bovio and P. Cecchi, *J. Organomet. Chem., 440* (1992) 27.

[5] S. Trofimenko, *J. Am. Chem. Soc., 89* (1967) 6288.

[6] (a) G.J. Long and B.B. Hutchinson, *Inorg. Chem., 26* (1987) 608; (b) S. Calogero, G. Gioia Lobbia, P. Cecchi, G. Valle and J. Friedl, *Polyhedron, 13* (1994) 87; (c) M. Bovens, T. Gerfin, V. Gramlich, W. Petter, L.M. Venanzi, M.T. Haward, S.A. Jackson and O. Eisenstein, *New J. Chem., 16* (1992) 337.

[7] F. Bonati, *Gazz. Chim. Ital., 119* (1989) 291.

[8] C. Lopez, R.M. Claramunt, D. Sanz, C. Foces-Foces, F.H. Cano, R. Faure, E. Cayon and J. Elguero, *Inorg. Chim. Acta, 176* (1990) 195.

[9] A. Bondi, *J. Phys. Chem., 68* (1964) 441.

[10] P. Cecchi, G. Gioia Lobbia, F. Marchetti, G. Valle and S. Calogero, *Polyhedron, 13* (1994) 2173.

[11] O.S. Jung, J.H. Jeong and Y.S. Sohn, *J. Organomet. Chem., 399* (1990) 235.

[12] B.K. Nicholson, *J. Organomet. Chem., 265* (1984) 153.

[13] D.H. O'Brien and C.-P. Hrung, *J. Organomet. Chem., 27* (1971) 185.

[14] The CS is a home made diffractometer by Colapietro and Spagna, prototype of that to be installed at ELETTRA synchrotron in Trieste, Italy.

[15] F. Bachechi, L. Zambonelli and G. Marcotrigiano, *J. Cryst. Mol. Struct. 7*, (1977) 11.

[16] N. Walker and D. Stuart, *Acta Crystallogr., Sect. A., 39* (1983) 158.

[17] F. Ugozzoli, *Comput. Chem., 11* (1987) 109.

[18] H.F. Allen, O. Kennard, D.G. Watson, L. Brammer and A.G. Orpen, *J. Chem. Soc., Perkin Trans., 2* (1987) S1.

[19] *International Tables for X-ray Crystallography*, Vol. IV, Kynoch, Birmingham, 1974, p. 99.

[20] M. Camalli, D. Capitani, G. Cascarano, S. Cerrini, C. Giacovazzo and R. Spagna, Italian Patent No 35403c/86. SIR CAOS user guide, Istituto di Strutturistica Chimica CNR.

[21] A. Altomare, G. Cascarano, C. Giacovazzo, A. Guagliardi, M.C. Burla, G. Polidori and M. Camalli, *J. Appl. Crystallogr., 27* (1994) 435.